Spur Reactions Observed by Picosecond Pulse Radiolysis in Highly Concentrated Bromide Aqueous Solutions

ARTICLE *in* THE JOURNAL OF PHYSICAL CHEMISTRY A · FEBRUARY 2013

Impact Factor: 2.69 · DOI: 10.1021/jp312023r · Source: PubMed

THE JOURNAL OF PHYSICAL CHEMISTRY A

Article

pubs.acs.org/JPCA

Spur Reactions Observed by Picosecond Pulse Radiolysis in Highly Concentrated Bromide Aqueous Solutions

Abdel Karim El Omar,[†] Uli Schmidhammer,[†] Anna Balcerzyk,[†] Jay LaVerne,[‡] and Mehran Mostafavi[†,*]

[†]Laboratoire de Chimie Physique/ELYSE, UMR 8000 CNRS, Université Paris-Sud 11, 91400 Orsay, France

[‡]Radiation Laboratory and Department of Physics, University of Notre Dame, Notre Dame, Indiana 46556, United States

ABSTRACT: The formation of the well-known product Br_3^-, observed in the steady-state radiolysis of highly concentrated Br^- aqueous solutions, has now been directly observed at ultrashort times corresponding to the relaxation of the spur. The transient absorption induced by picosecond pulse radiolysis of 6 M Br^- aqueous solution was probed simultaneously at 260 nm with the third harmonic laser wave and from 350 to 750 nm with a supercontinuum generated by the fundamental laser wave. This approach allows several transient radiolytic species to be followed in parallel, particularly the solvated electron, $BrOH^{-\bullet}$, $Br_2^{-\bullet}$, and Br_3^-. The kinetics measured within 4 ns at 260 and 370 nm clearly exhibit that the decay of $Br_2^{\bullet-}$ is correlated with the formation of Br_3^-. In highly concentrated Br^- solutions, the $OH^\bullet$ radical is fully replaced by $Br_2^{\bullet-}$, and the spur kinetics of $OH^\bullet$ radical in pure water is comparable with that of $Br_2^{-\bullet}$. Model calculations indicate that the main $OH^\bullet$ radical combination product H_2O_2 in pure water has formation kinetics similar to that of Br_3^- in 6 M Br^- solutions. Moreover, they point out that oxidation of Br^- occurs within the electron pulse both by direct energy absorption and by scavenging of the water radical cation, $H_2O^{\bullet+}$.

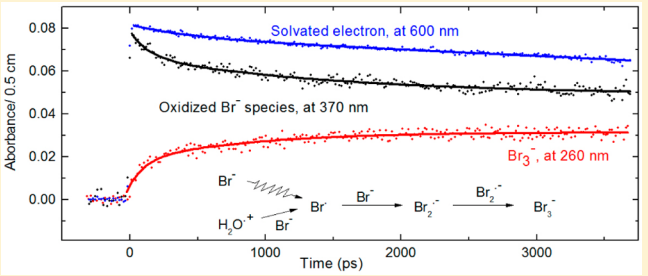

INTRODUCTION

The chemistry induced by radiation can be different in highly concentrated aqueous solutions compared to water and dilute solutions. Picosecond pulse−probe radiolysis of highly concentrated aqueous solutions up to 8 M chloride ions, Cl^-, clearly show that the amount of $Cl_2^{\bullet-}$ formation within the electron pulse increases notably with increasing Cl^- concentration.[1] The measurements reveal that the direct ionization of Cl^- cannot solely explain the significant amount of fast $Cl_2^{\bullet-}$ formation within the electron pulse. The results suggest that Cl^- reacts with the precursor of the $OH^\bullet$ radical, i.e., $H_2O^{\bullet+}$ radical, to form $Cl^\bullet$ atom within the electron pulse, and the $Cl^\bullet$ atom reacts subsequently with Cl^- to form $Cl_2^{\bullet-}$ on the very short time scales. Proton transfer reaction between $H_2O^{\bullet+}$ and the water molecule competes with the electron transfer reaction between Cl^- and $H_2O^{\bullet+}$. Molecular dynamics simulations point out that the number of hydrogen bonds between water molecules in the first shell decreases with increasing concentration of the salt, confirming that the proton transfer reaction between $H_2O^{\bullet+}$ with a water molecule becomes less efficient. Moreover, diffusion-kinetic simulations of spur reactions including the direct ionization of Cl^- and hole scavenging by Cl^- indicate that up to 30% of the $H_2O^{\bullet+}$ produced by the irradiation are scavenged for solutions containing 5.5 M Cl^-. This process decreases the yield of $OH^\bullet$ radical in solution on the picosecond time scale but increases the yield of $Cl_2^{\bullet-}$. The high yield of $Cl_2^{\bullet-}$ formation must favor the Cl_3^- formation in the spurs at short time. Since the extinction coefficient of this species is very weak in the UV, the subsequent $Cl_2^{\bullet-}$ disproportionation reaction in spurs cannot be followed at short times. Similar observations were also obtained in highly concentrated nitric acid in which a charge transfer between $H_2O^{\bullet+}$ and NO_3^- was assumed to explain the earliest formation of the $NO_3^\bullet$ radical.[2]

The radiolytic oxidation of bromide ions, Br^-, at low concentrations in aqueous solution is relatively well understood and involves several mechanisms. The γ-radiolysis of aerated aqueous solutions of potassium bromide, KBr, generates the tribromide ion, Br_3^-.[3] Microsecond pulse radiolysis studies established the mechanism and determined many of the rate constants for this system.[4−6] Later, this system was reexamined by nanosecond pulse radiolysis, and rate constants for the faster reactions were determined.[7] The absorption spectra of $Br_2^{-\bullet}$ and its reaction rate constant were reported not only at room temperature but also at higher temperatures.[8,9] Recently, γ-radiolysis studies on highly concentrated aqueous solutions of Br^- were performed to examine the total radical yield.[10,11] These studies found that in 6 M Br^-, around 40% of the dose is absorbed by the solute and Br^- is transformed to $Br^\bullet$. The precursors of Br_3^- are $BrOH^{\bullet-}$ and $Br_2^{\bullet-}$ and both of these species have absorption bands with significant extinction coefficients in the near UV. Picosecond pulse−probe radiolysis measurements were able to depict the mechanism of halide oxidation in highly concentrated aqueous solutions by

Received: December 6, 2012
Revised: February 20, 2013
Published: February 26, 2013

observing these transient species.[12] The interesting results are that not only are Br^- anions directly transformed into $Br^•$ by the electron pulse (direct effect) but they also can undergo prompt oxidation by water-related intermediates, possibly involving a hole in the coordination sphere of the solvated halide anions.

In the present study, the decay of the solvated electron is observed in the visible simultaneously with the oxidized species of Br^- in the UV at 370 and at 260 nm in order to follow the spur reactions in highly concentrated Br^- aqueous solutions. The yields of $Br_2^{•-}$ and Br_3^- are deduced from the kinetics and the mechanism of Br^- oxidation is established. Model simulations of the radiolysis of 6 M Br^- aqueous solution are used to clarify how the spur reactions are modified when the precursor of $OH^•$ radical is scavenged by Br^-. Finally, a comparison of the kinetics in 6 M Br^- solution with those in pure water is used to describe the formation of H_2O_2 in pure water radiolysis.

EXPERIMENTAL SECTION

The working principle and parameters of ELYSE, a picosecond electron accelerator based on the radiofrequency photogun technology, are detailed elsewhere.[13,14] The electron energy was set to 7 MeV and the pulse charge to 4 nC (± 10%) at a repetition rate of 10 Hz. The basics of the electron pump optical probe absorption setup with typical parameters of measurement and data acquisition can be found in reference 15. Both the electron and the optical pulses are generated by the same femtosecond laser source, a chirped pulse amplification Ti:Sapphire laser (pulse duration 100 fs, center wavelength ∼ 782 nm), and are therefore intrinsically synchronized. The main part of the available energy is frequency tripled and seeded into the photogun. Before the third harmonic generation unit a beam splitter separates several 100 μJ that can be used for the generation of the probe pulses.

The optical configuration that allows simultaneous measurement in the middle UV at 260 nm and in the near UV to near-infrared is detailed in ref 16 including the multichannel detection scheme. Shortly, after passing the optical delay line, the laser beam is split into two parts that are arranged in a rectangle. In one arm of the rectangle, a supercontinuum was generated in a CaF_2 disk to probe the absorbance changes from 350 to 750 nm. In the second arm of the rectangle, the third harmonic of the initial laser wavelength is generated. After filtering the initial laser waves, the supercontinuum and the third harmonic probe beams are unified by a 50% beam splitter to propagate on a common optical path through the sample cell toward the detector unit, a polychromator and a CCD.

The samples were placed 30 mm away from the output window of the ELYSE vacuum tube and behind a 200 μm thin aluminum mirror. The latter was used to direct the optical probe beams collinear with the electron beam through the cell. The diameter of the electron bunch at the position of the cell was in the range of 3−4 mm, the supercontinuum and the third laser harmonic beams were on the scale of 100 μm. The spatial overlap of the electron beam on the probe beams was optimized using the transient absorption signal of water. Under the described settings of the accelerator and at the position of the optical cell, single shot electro-optic sampling of the electric field copropagating with the relativistic electron bunch revealed a pulse duration around 10 ps and a rms shot-to-shot jitter < 1 ps.[17,18] The dose per pulse in pure water was determined by measuring the absorbance of the solvated electron, $A_{e^-_{aq}}(\lambda, t)$ and by considering its initial yield measured at 10 ps to be $G(t = 10\ \text{ps}) = 4.25 \times 10^{-7}$ mol J^{-1}.[19] Therefore, the dose absorbed in water is given by

$$D_{\text{water}}\ (\text{Gy}) = \frac{A_{e^-_{hyd}}(\lambda, t)}{\varepsilon_\lambda l \rho_w G(t)} \quad (1)$$

where ε is the solvated electron extinction coefficient (19 130 M^{-1} cm^{-1}, at maximum 718 nm),[20] l is the optical path length inside the flow cell (5 mm), and ρ_w is the density of water. The absorbance measured for a given species in highly concentrated solutions is given by eq 2:

$$A(\lambda, t) = \varepsilon_\lambda l c(t) = \varepsilon_\lambda l F D_W G(t) \quad (2)$$

The overall dose that takes into account the dose additionally absorbed by the solute in concentrated solutions is obtained by multiplying the absorbed dose in pure water by the dose factor F:

$$F = \rho_{\text{sol}}(Z_{\text{NaBr}}p/A_{\text{NaBr}} + Z_{\text{water}}(100 - p)/A_{\text{water}})\ (Z_{\text{water}}100/A_{\text{water}})^{-1} \quad (3)$$

where ρ_{sol} is the density of the solution, Z is the number of electrons, A is the mass number, and p is the weight fraction of the solute per 100 g of solution. Solutions containing halide anions at high concentration and pure water were studied under identical experimental conditions. Particular attention was given to the use of a constant dose per pulse. The pulse radiolysis measurements were performed at 22.5 °C.

The transient absorption induced in the fused silica optical cell is not negligible[16] and was measured under identical conditions with the described pump probe technique in the UV and visible range. The kinetics recorded in solutions were corrected for this contribution of the fused silica windows in order to avoid important errors on the time dependent yield of transient species, particularly of those absorbing in the UV.

The chemical reagents were purchased from Sigma-Aldrich. The purity of NaBr was greater than 99.9%. Water was purified by passage through a Millipore purification system. The solutions were air saturated, and they were prepared at pH 6. The solutions containing halide anions at high concentration and neat water were studied under identical experimental conditions. The temporal evolution of each sample under investigation was scanned on the order of 10 times with a single point averaging of 5 to 20 for each delay step.

DIFFUSION-KINETIC METHODOLOGY

The chemistry of an isolated spur with Br^- as the solute was examined in exactly the same manner as previously done with Cl^- solutions.[1] This method employs a nonhomogeneous deterministic model in which the coupled differential equations for the various reactions were stepped in time using FACSIMILE, which is based on the Gear algorithm.[21] Water reactions, rate coefficients, and diffusion coefficients are the same as used previously.[1,22] The initial Gaussian spatial distributions were normalized using neat water radiolysis to give reasonable agreement with the reported yields of 4.8×10^{-7} mol J^{-1} for the $OH^•$ radical at 10 ps and 4.2×10^{-7} mol J^{-1} for the hydrated electron at 10 ps and by matching the observed decay of these two species in pure water up to 1 μs.[1,19] Goodness of fit of the pure water reactions to the available data can be observed in the previous work.[1] Modeling

dx.doi.org/10.1021/jp312023r | J. Phys. Chem. A 2013, 117, 2287−2293

the oxidation of Br^- was performed by including the reaction scheme listed in Table 1. Rate coefficients for each of the Br^-

Table 1. Reaction Scheme Used for the Oxidation of Br^-

	reaction	k (M^{-1} s^{-1}) or (s^{-1})
R1	$OH^\bullet + Br^- \rightarrow BrOH^{\bullet-}$	1.1×10^{10}
R2	$BrOH^{\bullet-} \rightarrow OH^\bullet + Br^-$	3.3×10^{7}
R3	$H^+ + BrOH^{\bullet-} \rightarrow Br^\bullet + (H_2O)$	4.4×10^{10}
R4	$BrOH^{\bullet-} \rightarrow Br^\bullet + OH^-$	4.2×10^{6}
R5	$Br^\bullet + OH^- \rightarrow BrOH^{\bullet-}$	1.3×10^{10}
R6	$Br^\bullet + Br^- \rightarrow Br_2^{\bullet-}$	1.2×10^{10}
R7	$Br_2^{\bullet-} \rightarrow Br^\bullet + Br^-$	1.9×10^{4}
R8	$Br_2^{\bullet-} + Br_2^{\bullet-} \rightarrow Br_3^- + Br^-$	2.4×10^{9}
R9	$Br^\bullet + Br_2^{\bullet-} \rightarrow Br_3^-$	5.0×10^{9}
R10	$Br^- + Br_2 \rightarrow Br_3^-$	1.6×10^{8}
R11	$Br_3^- \rightarrow Br^- + Br_2$	1.0×10^{7}
R12	$Br^\bullet + Br^\bullet \rightarrow Br_2$	5.0×10^{9}
R13	$e_{sol}^- + Br^\bullet \rightarrow Br^-$	1.0×10^{10}
R14	$e_{sol}^- + Br_2^{\bullet-} \rightarrow 2Br^-$	1.3×10^{10}
R15	$e_{sol}^- + Br_3^- \rightarrow Br^- + Br_2^{\bullet-}$	2.7×10^{10}
R16	$H^\bullet + Br^\bullet \rightarrow H^+ + Br^-$	1.0×10^{10}
R17	$H^\bullet + Br_2^{\bullet-} \rightarrow H^+ + 2Br^-$	1.4×10^{10}
R18	$H^\bullet + Br_3^- \rightarrow H^+ + Br^- + Br_2^{\bullet-}$	1.2×10^{10}
R19	$HO_2^\bullet + Br_2^{\bullet-} \rightarrow 2Br^- + O_2 + H^+$	1.0×10^{8}
R20	$HO_2^\bullet + Br_3^- \rightarrow Br_2^{\bullet-} + Br^- + O_2 + H^+$	1.0×10^{7}
R21	$BrOH^{\bullet-} + Br^- \rightarrow Br_2^{\bullet-} + OH^-$	1.9×10^{8}
R22	$Br_2^{\bullet-} + OH^- \rightarrow BrOH^{\bullet-} + Br^-$	2.7×10^{6}
R23	$H + Br^- \rightarrow HBr^-$	1.7×10^{6}
R24	$H^+ + HBr^- \rightarrow H_2 + Br^\bullet$	1.1×10^{10}

oxidation reactions were as given in the literature. The diffusion coefficients used were 2.1, 1.2, 1.1, 1.1, and 1.1×10^{-5} cm^2/s for $Br^\bullet$, $Br_2^{\bullet-}$, Br_3^-, $BrOH^{\bullet-}$, and Br_2, respectively.

No attempt was made to model subpicosecond kinetics because of inherent limitations in the approach. The direct ionization of Br^- to give $Br^\bullet$ and e_{sol}^- was assumed to be proportional to the electron fraction of this component in the solution. The radiation chemical yield for this process was assumed to be the same as for the ionization of water. Electron fractions were obtained from the molarities of the solutions, and the values are given in Table 2. Scavenging of the $H_2O^{\bullet+}$ by Br^- to give $Br^\bullet$ was also not directly modeled but rather assumed to occur at some predetermined amount chosen to best match the experimental results. The yield of $Br^\bullet$ formed by direct ionization of Br^- or by scavenging of $H_2O^{\bullet+}$ was included in the initial (1 ps) yields and the amount of initial $OH^\bullet$ radical adjusted appropriately.

RESULTS

Table 2 contains the values of the dose factor F, the electron density fractions of solute and water (f_s and f_w, respectively), as well as water concentration. The normalized spectra of solvated electron in pure water (red dots) and in 6 M NaBr (blue dots) solutions are reported in the left inset of Figure 1. The additional absorption band peaking around 370 nm is due to $BrOH^{\bullet-}$ and $Br_2^{\bullet-}$. The maximum of absorbance of the

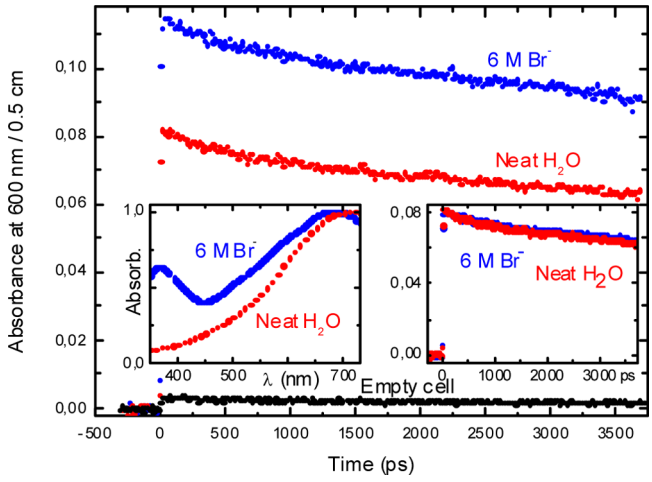

Figure 1. Decay kinetics observed at 600 nm in neat water and 6 M Br^- solutions (red and blue dots, respectively) as well as the contribution of the fused silica window (black dots). The left inset figure shows the spectrum of solvated electrons in the presence of Na^+ cations compared to that in neat water as well as the absorption peak at ~370 nm, which is the signature of oxidized species of Br^-. The right inset shows the decay kinetics observed at 600 nm in neat water and 6 m Br^- solutions after consideration of the spectral shift and normalization by the dose factor.

solvated electron in water is located at 718 nm while it is blue-shifted over 35 nm in presence of 6 M NaBr. This result is in good agreement with the previous work performed on Na^+ solutions using nanosecond pulse radiolysis.[23,24] The blue shift in the spectrum is due to the electrostatic interaction between the solvated electron and the Na^+ cation.[23−25] Figure 1 also shows the kinetics of solvated electrons in both media recorded at 600 nm: the shape of the decay of the solvated electron is the same yet the absorbance is higher when the salt is present. This increase of absorbance at 600 nm is due to the blue shift of the solvated electron absorption (causing a higher extinction coefficient at this wavelength than in pure water) and the increase of absorbed dose by the direct radiation effect on the solute. Taking into account the change of extinction coefficient due to the spectral shift and normalizing with the dose factor F according to eqs 2 and 3, the transient absorption signal, i.e., amplitude and shape, are identical for neat water and the solution containing 6 M Br^- (Figure 1, inset to the right). This result is clear evidence regarding the direct effect of ionizing radiations on the solute itself and points out that the yields of electrons detached from Br^- and that from a water molecule are close. Figure 2 shows the kinetic decay trace obtained at 370 nm in the presence of 6 M Br^-. Different species absorb at this wavelength. The irradiation of NaBr solutions leads to the formation of the oxidized species $BrOH^{\bullet-}$ and $Br_2^{\bullet-}$ absorbing at 370 nm. The extinction coefficients of $Br_2^{\bullet-}$ and $BrOH^{\bullet-}$ at 370 nm are found to be 8840 and 7742 M^{-1} cm^{-1}, respectively.[8] In addition to these species, e_{sol}^-, as well as the transient induced in the fused silica windows of the flow cell, absorbs at 370 nm, and their contribution to the absorption is shown in Figure 2. The extinction coefficient of Br_3^- at this

Table 2. Chemical Composition of Aqueous 6 M Bromide Solution Studied by Picosecond Pulse Radiolysis

solution	Br^- (mol dm^{-3})	water (mol dm^{-3})	density (kg dm^{-3})	F kg dm^{-3}	f_s	f_w
NaBr	6	43.48	1.4	1.3	0.38	0.62

dx.doi.org/10.1021/jp312023r | J. Phys. Chem. A 2013, 117, 2287−2293

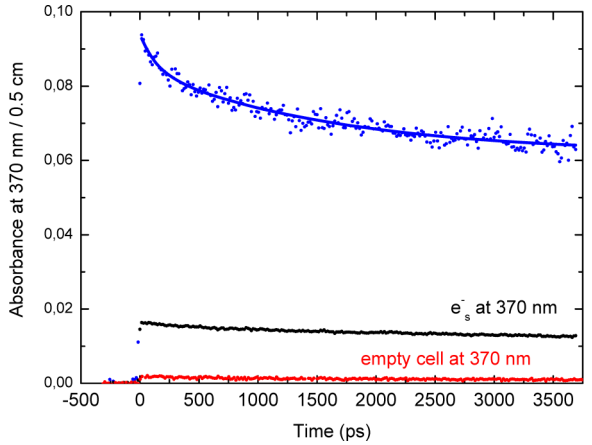

Figure 2. Decay kinetics observed at 370 nm in 6 M Br^- solution. The contributions of solvated electron absorbance and transients in fused silica windows are also shown. The lines are a guide to the eyes.

wavelength is only 740 M^{-1} cm^{-1}, i.e., more than 15 times lower than those of $BrOH^{-\bullet}$ or $Br_2^{-\bullet}$. Figure 3 shows the

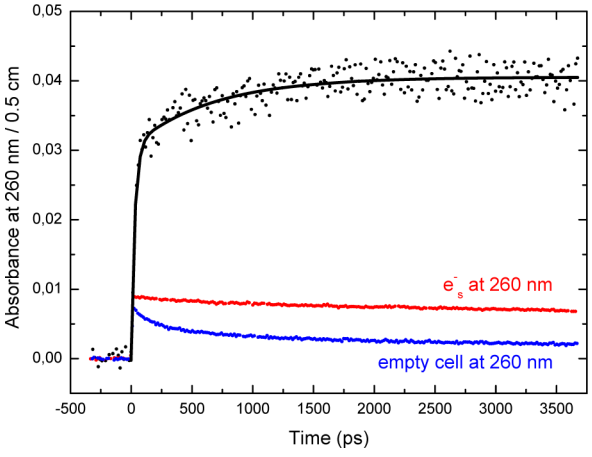

Figure 3. Kinetics observed at 260 nm in 6 M Br^- solution. The contributions of solvated electron absorbance and transients in fused silica windows are also shown. The lines are a guide to the eyes.

kinetics at 260 nm in 6 M Br^- that can be mainly attributed to the formation of Br_3^-, which is the stable product of Br^- irradiated solution. The maximum of absorbance of Br_3^- is located at 265 nm. Figure 3 shows also the contributions of e_{sol}^- and the transient induced in fused silica windows that are both absorbing at 260 nm. The signal of the solvated electron is deduced from that at 600 nm, and the signal due to the fused silica windows is from the fit of the kinetics observed in an empty cell at 260 nm in our previous work.[16]

The different kinetics obtained at 370 and 260 nm were then regrouped after normalization with the dose factor F and subtraction of the contribution of the solvated electron and the fused silica windows (Figure 4). Finally, the transient absorption kinetics of Br_3^- formation as given in Figure 4 was divided by the absorbed dose (28.6 Gy), the molar absorption coefficient at 260 nm, and the optical path length to give the time dependent formation yield of Br_3^- as shown in Figure 5.

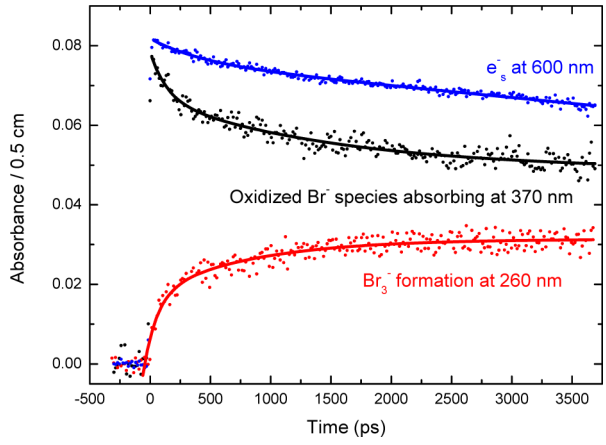

Figure 4. Kinetics of the decay of solvated electrons, of Br^- oxidized species, and of the formation of Br_3^- observed at 600, 370, and 260 nm, respectively, in 6 M Br^- solution (after subtraction of the contribution of transients induced in fused silica cell for each kinetic decay and that of the solvated electron for kinetics at 370 and 260 nm). The lines are guide to the eyes.

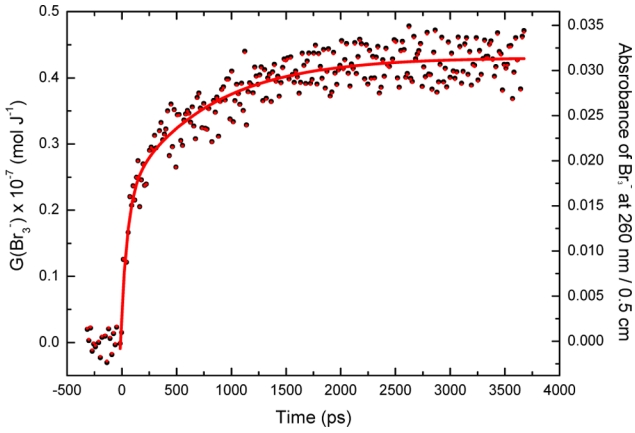

Figure 5. Time dependent radiolytic formation yield of Br_3^- in 6 M Br^- solution.

DISCUSSION

The results of Figure 4 clearly show that the oxidized species of Br^- at 370 nm are decaying while Br_3^- is being formed simultaneously, which suggests a very fast formation process for the latter. The formation of Br_3^- increases until it reaches a plateau at around 3.5 ns after the electron pulse with a radiolytic yield of 0.43×10^{-7} mol J^{-1}. Possible modes for the formation of Br_3^- are given by reactions R8 and R9, and both reactions involve $Br_2^{\bullet-}$ as the precursor. Reaction R9 is a scavenging of the $Br^\bullet$ atom while R8 is a disproportionation reaction. The observation of Br_3^- at short time shows that an important amount of $Br_2^{\bullet-}$ must be present at the end of the electron pulse. However, diffusion processes are much too slow for the standard reactions shown in Table 1 to occur on this time scale. In the presence of high concentrations of solute, the dose is absorbed by water and by the solute itself; thus, a correction must be taken into account by considering the density of the solution as well as the electronic concentration of both solvent and solute.[26] Direct absorption of energy by the solute leads to the formation of very reactive species at short times with the electron pulse. Reaction of these species with

dx.doi.org/10.1021/jp312023r | J. Phys. Chem. A 2013, 117, 2287−2293

normal water decomposition products and with added solutes can greatly modify the kinetics.

The initial absorbance observed at 10 ps at 370 nm can be considered to be due to the fast formation of $Br_2^{\bullet-}$ (R6) and the scavenging of $OH^\bullet$ radicals by Br^- forming $BrOH^{\bullet-}$ (R1). Since the oxidation yield of Br^- is due to both direct and indirect effect, it can be expressed in the following form.

$$G_{ox}^{Br^-} = f_s G_s + f_w G_w \quad (4)$$

The values for both f_s and f_w are reported in Table 1, and G_s and G_w are the ionization yields of the solute and water, respectively. Direct absorption of the ionizing radiation leads to the formation of $Br^\bullet$ and an electron. As we reported above, the radiolytic yield of this latter species, G_s, is equal to that of $G(e_{sol}^-)$. When the concentration of Br^- is 6 M, the reaction of Br^- with $Br^\bullet$ ($t_{1/2}$ = ln 2/(6 mol dm^{-3} × 1.2 × 10^{10} dm^3 mol^{-1} s^{-1}) = 9.6 ps) occurs within the experimental time resolution of about 20 ps. For the indirect effect, the maximum value of G_w must be assumed to be equal to the value of $G(OH^\bullet)$ = 4.85 × 10^{-7} mol J^{-1}, which was determined in a previous study.[27] Thus, by considering the direct effect on Br^- and the scavenging of all $OH^\bullet$ radicals, the expected value of the maximum of the absorbance at 370 nm after the pulse is

$$A_{t=10ps}^{370nm} = FlD(0.38 \times 4.25 \times 10^{-7} \times \varepsilon_{Br_2^{\bullet-}}^{370nm} + 0.62 \times 4.85 \times 10^{-7} \times \varepsilon_{BrOH^{\bullet-}}^{370nm}) = 0.069 \quad (5)$$

However, this value is still lower than that observed (0.078), which suggests another contribution to the formation of $Br_2^{\bullet-}$.

As reported recently in highly concentrated halide solutions, scavenging of the positive hole, $H_2O^{\bullet+}$, competes with the proton transfer reaction and can also contribute to the fast formation of $Br_2^{\bullet-}$. Direct ionization of water leads to the formation of the $H_2O^{\bullet+}$ radical cation within the electron pulse. The $H_2O^{\bullet+}$ radical is a highly oxidizing species, and the proton transfer between $H_2O^{\bullet+}$ and H_2O usually occurs within 100 fs in neat water. Even if the proton transfer is ultrafast in neat water (a value of around 10 fs is reported for the proton transfer reaction[28,29]), the probability of this reaction is reduced just by decrease of water molecules in contact of $H_2O^{\bullet+}$ in solutions of 6 M Br^- (total 12 M cations and anions). Considering that NaBr is fully dissociated, there are only 3.6 water molecules per ion present in solution. Even if some part of Na^+ and Br^- are associated as contact ions pairs, then each water molecule is in close proximity to a cation or an anion and a direct charge transfer from Br^- to $H_2O^{\bullet+}$ is highly probable. This charge transfer reaction leads to the formation of $Br^\bullet$, which is quickly converted within the pulse into $Br_2^{\bullet-}$. Such a mechanism implies that considerably fewer $OH^\bullet$ radicals are formed in 6 M Br^- than in pure water and that these radicals do not make a large contribution to the oxidation of Br^-.

Diffusion−kinetic simulations of the spur reactions were performed to match the kinetics observed at 370 and 260 nm with the appropriate mechanisms. Even a complete reaction scheme as presented in Table 1 is not sufficient for matching the observed kinetics of the oxidized Br^- products. A direct ionization process of Br^- to give $Br^\bullet$ was included as based on the solute fraction given in Table 2. This process gave improved short time kinetics but was still insufficient to agree with the observations. A satisfactory match to the experimental data was found when direct scavenging of the $H_2O^{\bullet+}$ by Br^- was included. Almost 60% of the $H_2O^{\bullet+}$ may be scavenged in 6 M Br^- solutions. Such a large scavenging fraction is justified on the kinetics and by consideration of the nearest neighbors associated with water in 6 M Br^- solutions. Water radiolysis is obviously quite perturbed in highly concentrated solutions.

Direct observations of the solvated electron decay show that its kinetics is almost identical in neat water and in 6 M Br^- solutions. The main spur reaction in neat water involves the solvated electron and the $OH^\bullet$ radical. Formation of $Br_2^{-\bullet}$ in 6 M Br^- solution occurs almost within the electron pulse and consumes almost all of the $OH^\bullet$ radicals and its precursor. Since $Br_2^{\bullet-}$ is an oxidizing species it can be thought of as a pseudo $OH^\bullet$ radical. Figure 6 shows that the model calculation

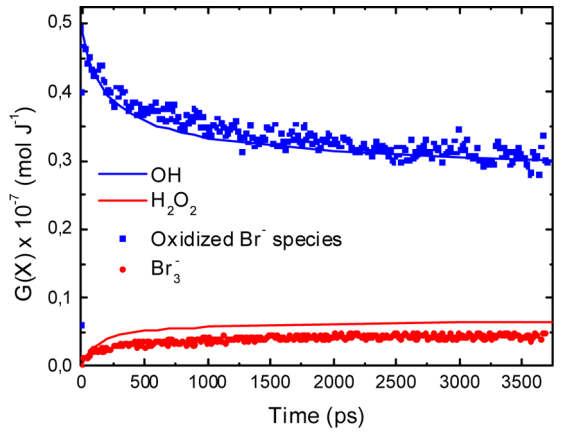

Figure 6. Experimental kinetics of the decay of the oxidized Br^- species ($BrOH^{-\bullet}$ and $Br_2^{-\bullet}$) and of the formation of Br_3^- compared with the model results (solid lines) predicted for the $OH^\bullet$ radical and H_2O_2 in neat water.

results for the $OH^\bullet$ radical in neat water agree well with the observations of the $Br_2^{\bullet-}$ decay in 6 M Br^- solutions. Previous studies have already shown that the model results for the $OH^\bullet$ radical kinetics in neat water match well with the direct, experimental observations.[1] Other than reaction with the solvated electron and $H^\bullet$ atom, the main reaction of $OH^\bullet$ radicals in neat water is a combination reaction to produce H_2O_2. A similar combination reaction, R8, of $Br_2^{\bullet-}$ is expected to occur in 6 M Br^- solutions to give Br_3^-. Direct observation of H_2O_2 transient kinetics is difficult because its extinction coefficient is very low and far in the UV, but the model predictions for its formation are shown in Figure 6 in comparison with that for Br_3^- in 6 M Br^- solution. The initial formation of H_2O_2 can be seen to match well with that for Br_3^- with a slight difference in the final plateau value. A confirmation of the formation rate of H_2O_2 is gratifying since its formation kinetics in spurs is not reported in literature and this species is an important component in the radiolysis of water. Moreover, the difference between the kinetics of Br_3^- and H_2O_2 is due to the fact that in 6 M Br^- solution a small amount of $BrOH^{\bullet-}$ is still present at one nanosecond, and this species does not follow a combination reaction to yield directly Br_3^-.

SUMMARY

Previous steady-state radiolysis studies have shown that the main oxidized product in the radiolysis of concentrated Br^- solutions is Br_3^-. This work presents the first direct observation of the oxidation of Br^- at the very short times corresponding to the relaxation of the spur. Picosecond electron pulse radiolysis is performed on a 6 M Br^- aqueous solution probing

dx.doi.org/10.1021/jp312023r | J. Phys. Chem. A 2013, 117, 2287−2293

simultaneously at 260 nm and from 350 to 750 nm. The resulting simultaneous observation of the solvated electron and the oxidized Br^- products is important to establish dosimetry and absolute yields. The kinetic measurements within 4 ns at 260 and 370 nm clearly show that the decay of $Br_2^{\bullet-}$ is correlated with the formation of Br_3^-. Model calculations point out that oxidation of Br^- occurs within the electron pulse both by direct energy absorption and by scavenging of the water radical cation, $H_2O^{\bullet+}$. Up to 60% of the $H_2O^{\bullet+}$ may be scavenged before proton transfer to water can occur. This path is possible because of the very strong correlation of each water molecule with an ion species in 6 M Br^- solutions. In the highly concentrated Br^- solution, the $OH^\bullet$ radical is fully replaced by $Br_2^{\bullet-}$ and the spur kinetics of $OH^\bullet$ radical in pure water is comparable with that of $Br_2^{\bullet-}$ in 6 M Br^- solutions. The main $OH^\bullet$ radical combination product H_2O_2 in pure water is shown to have formation kinetics similar to that of Br_3^- in 6 M Br^- solutions.

AUTHOR INFORMATION

Corresponding Author

*E-mail: mehran.mostafavi@u-psud.fr.

Notes

The authors declare no competing financial interest.

ACKNOWLEDGMENTS

J.L. is thankful for the support of the University of Paris-Sud for a visiting position to develop the diffusion-kinetic model. His research described herein was also supported through the Division of Chemical Sciences, Geosciences and Biosciences, Basic Energy Sciences, Office of Science, United States Department of Energy, through Grant No. DE-FC02-04ER15533. This is Contribution No. NDRL 4946 from the Notre Dame Radiation Laboratory.

REFERENCES

(1) El Omar, A. K.; Schmidhammer, U.; Rousseau, B.; LaVerne, J.; Mostafavi, M. Competition Reactions of H2O●+ Radical in Concentrated Cl− Aqueous Solutions: Picosecond Pulse Radiolysis Study. *J. Phys. Chem. A* **2012**, *116* (47), 11509−11518.

(2) Balcerzyk, A.; El Omar, A. K.; Schmidhammer, U.; Pernot, P.; Mostafavi, M. Picosecond Pulse Radiolysis Study of Highly Concentrated Nitric Acid Solutions: Formation Mechanism of NO3● Radical. *J. Phys. Chem. A* **2012**, *116* (27), 7302−7307.

(3) Rafi, A.; Sutton, H. C. Radiolysis of Aerated Solutions of Potassium Bromide. *Trans. Faraday Soc.* **1965**, *61* (0), 877−890.

(4) Matheson, M. S.; Mulac, W. A.; Weeks, J. L.; Rabani, J. The Pulse Radiolysis of Deaerated Aqueous Bromide Solutions1. *J. Phys. Chem.* **1966**, *70* (7), 2092−2099.

(5) Zehavi, D.; Rabani, J. Oxidation of Aqueous Bromide Ions by Hydroxyl Radicals. Pulse Radiolytic Investigation. *J. Phys. Chem.* **1972**, *76* (3), 312−319.

(6) Mamou, A.; Rabani, J.; Behar, D. On the Oxidation of Aqueous Br- by OH Radicals, Studied by Pulse Radiolysis. *J. Phys. Chem.* **1977**, *81* (15), 1447−1448.

(7) D'Angelantonio, M.; Venturi, M.; Mulazzani, Q. G. A Re-Examination of the Decay Kinetics of Pulse Radiolytically Generated Br-2 Radicals in Aqueous Solution. *Int. J. Radiat. Appl. Instrum., Part C: Radiat. Phys. Chem.* **1988**, *32* (3), 319−324.

(8) Lampre, I.; Marignier, J.-L.; Mirdamadi-Esfahani, M.; Pernot, P.; Archirel, P.; Mostafavi, M. Oxidation of Bromide Ions by Hydroxyl Radicals: Spectral Characterization of the Intermediate BrOH●−. *J. Phys. Chem. A* **2013**, *117* (5), 877−887.

(9) Lin, M.; Archirel, P.; Van-Oanh, N. T.; Muroya, Y.; Fu, H.; Yan, Y.; Nagaishi, R.; Kumagai, Y.; Katsumura, Y.; Mostafavi, M. Temperature Dependent Absorption Spectra of Br−, Br2●−, and Br3− in Aqueous Solutions. *J. Phys. Chem. A* **2011**, *115* (17), 4241−4247.

(10) Mirdamadi-Esfahani, M.; Lampre, I.; Marignier, J.-L.; de Waele, V.; Mostafavi, M. Radiolytic Formation of Tribromine Ion Br3− in Aqueous Solutions, a System for Steady-State Dosimetry. *Radiat. Phys. Chem.* **2009**, *78* (2), 106−111.

(11) Balcerzyk, A.; LaVerne, J.; Mostafavi, M. Direct and Indirect Radiolytic Effects in Highly Concentrated Aqueous Solutions of Bromide. *J. Phys. Chem. A* **2011**, *115* (17), 4326−4333.

(12) Balcerzyk, A.; Schmidhammer, U.; El Omar, A. K.; Jeunesse, P.; Larbre, J.-P.; Mostafavi, M. Picosecond Pulse Radiolysis of Direct and Indirect Radiolytic Effects in Highly Concentrated Halide Aqueous Solutions. *J. Phys. Chem. A* **2011**, *115* (33), 9151−9159.

(13) Belloni, J.; Monard, H.; Gobert, F.; Larbre, J. P.; Demarque, A.; De Waele, V.; Lampre, I.; Marignier, J. L.; Mostafavi, M.; Bourdon, J. C.; et al. Elyse—a Picosecond Electron Accelerator for Pulse Radiolysis Research. *Nucl. Instrum. Methods Phys. Res., Sect. A* **2005**, *539* (3), 527−539.

(14) Marignier, J. L.; de Waele, V.; Monard, H.; Gobert, F.; Larbre, J. P.; Demarque, A.; Mostafavi, M.; Belloni, J. Time-Resolved Spectroscopy at the Picosecond Laser-Triggered Electron Accelerator Elyse. *Radiat. Phys. Chem.* **2006**, *75* (9), 1024−1033.

(15) Schmidhammer, U.; Pernot, P.; Waele, V.; Jeunesse, P.; Demarque, A.; Murata, S.; Mostafavi, M. Distance Dependence of the Reaction Rate for the Reduction of Metal Cations by Solvated Electrons: A Picosecond Pulse Radiolysis Study. *J. Phys. Chem. A* **2010**, *114* (45), 12042−12051.

(16) Schmidhammer, U.; El Omar, A. K.; Balcerzyk, A.; Mostafavi, M. Transient Absorption Induced by a Picosecond Electron Pulse in the Fused Silica Windows of an Optical Cell. *Radiat. Phys. Chem.* **2012**, *81* (11), 1715−1719.

(17) Schmidhammer, U.; De Waele, V.; Marquès, J. R.; Bourgeois, N.; Mostafavi, M. Single Shot Linear Detection of 0.01−10 Thz Electromagnetic Fields. *Appl. Phys. B: Laser Opt.* **2009**, *94* (1), 95−101.

(18) De Waele, V.; Schmidhammer, U.; Marquès, J.-R.; Monard, H.; Larbre, J.-P.; Bourgeois, N.; Mostafavi, M. Non-Invasive Single Bunch Monitoring for Ps Pulse Radiolysis. *Radiat. Phys. Chem.* **2009**, *78* (12), 1099−1101.

(19) Muroya, Y.; Lin, M.; Wu, G.; Iijima, H.; Yoshii, K.; Ueda, T.; Kudo, H.; Katsumura, Y. A Re-Evaluation of the Initial Yield of the Hydrated Electron in the Picosecond Time Range. *Radiat. Phys. Chem.* **2005**, *72* (2−3), 169−172.

(20) Jou, F.-Y.; Freeman, G. R. Shapes of Optical Spectra of Solvated Electrons. Effect of Pressure. *J. Phys. Chem.* **1977**, *81* (9), 909−915.

(21) Chance, E. M.; Curtis, A. R.; Jones, I. P.; Kirby, C. R. *Facsimile: A Computer Program for Flow and Chemistry Simulation, and General Initial Value Problems*; Harwell: AEA Technology, 1977.

(22) LaVerne, J. A.; Pimblott, S. M. Scavenger and Time Dependences of Radicals and Molecular Products in the Electron Radiolysis of Water: Examination of Experiments and Models. *J. Phys. Chem.* **1991**, *95* (8), 3196−3206.

(23) Anbar, M.; Hart, E. J. The Effect of Solvent and of Solutes on the Absorption Spectrum of Solvated Electrons1a. *J. Phys. Chem.* **1965**, *69* (4), 1244−1247.

(24) Wolff, R. K.; Aldrich, J. E.; Penner, T. L.; Hunt, J. W. Picosecond Pulse Radiolysis. V. Yield of Electrons in Irradiated Aqueous Solution with High Concentrations of Scavenger. *J. Phys. Chem.* **1975**, *79* (3), 210−219.

(25) Bonin, J.; Lampre, I.; Mostafavi, M. Absorption Spectrum of the Hydrated Electron Paired with Nonreactive Metal Cations. *Radiat. Phys. Chem.* **2005**, *74* (5), 288−296.

(26) Pucheault, J.; Ferradini, C.; Julien, R.; Deysine, A.; Gilles, L.; Moreau, M. Radiolysis of Concentrated Solutions. 1. Pulse And .Gamma. Radiolysis Studies of Direct and Indirect Effects in Lithium Chloride Solutions. *J. Phys. Chem.* **1979**, *83* (3), 330−336.

(27) El Omar, A. K.; Schmidhammer, U.; Jeunesse, P.; Larbre, J.-P.; Lin, M.; Muroya, Y.; Katsumura, Y.; Pernot, P.; Mostafavi, M. Time-

Dependent Radiolytic Yield of OH• Radical Studied by Picosecond Pulse Radiolysis. *J. Phys. Chem. A* **2011**, *115* (44), 12212−12216.
(28) De Waele, V.; Lampre, I.; Mostafavi, M. Time-Resolved Study on Nonhomogeneous Chemistry Induced by Ionizing Radiation with Low Linear Energy Transfer in Water and Polar Solvents at Room Temperature. In *Charged Particle and Photon Interactions with Matter*; Hatano, Y., Katsumura, Y., Mozumder, A., Eds.; CRC Press: New York, 2010; pp 289−324.
(29) Garrett, B. C.; Dixon, D. A.; Camaioni, D. M.; Chipman, D. M.; Johnson, M. A.; Jonah, C. D.; Kimmel, G. A.; Miller, J. H.; Rescigno, T. N.; Rossky, P. J.; et al. Role of Water in Electron-Initiated Processes and Radical Chemistry: Issues and Scientific Advances. *Chem. Rev.* **2005**, *105* (1), 355−390.